

FORMATION OF COMPOSITE COATINGS BY ELECTROCHEMICAL CO-DEPOSITION OF GOLD AND CARBON NANOCAPSULES

N. Alonso-Morales¹, Igual Muñoz², J. Palomar¹, M. A. Gilarranz¹, S. Mischler²

¹ Chemical Engineering Department, Autónoma University of Madrid, Madrid, Spain

² Ecole Polytechnique Fédérale de Lausanne, Tribology and Interface Chemistry Group, CH-1015 Lausanne, Switzerland

*noelia.alonso@uam.es

Introduction

Composite coatings formed by electrolytic co-deposition of inert, semi-conductive, and conductive particles with metal from galvanic baths has received great attention due to improved mechanical and physicochemical properties of the resulting material, i.e. corrosion and wear resistance, and the variety of engineering applications (aerospace, sensors, automotive, electronics, memory devices, construction, energy, biomedical, etc.)¹. The type, size and number of incorporated particles depends on the final functionality desired for the composite coating. Among different particles, carbon is one of the first materials whose co-deposition was reported in literature², probably due to the combination of hydrophobicity and conductivity. Gold electrodeposition is widely used, however, lifetime of gold coatings is still a concern and the increase in durability of those gold coatings could be improved by incorporating solid particles into the metallic matrix. Different particles have been successfully incorporated to gold and gold alloy coatings via electrochemical co-deposition (PTFE, ceramics, carbons...)³. This work is focus carbon nanocapsules as acting as carriers for the further development of smart coatings⁴.

Materials and Methods

Synthesis of carbon nanocapsules and suspension preparation. The carbon nanocapsules were synthesized following the templating method⁵⁻⁷. The silica templates were synthesized using tetraethylorthosilicate (TEOS) as silica precursor and octadecyltrimethoxysilane (C18TMS) as porogenic agent in a two-step procedure: firstly the solid core was formed, and secondly a porous shell was synthesized around the core. The template particles synthesized were isolated by filtration and calcined under air. A commercial resol resin was infiltrated into the silica template and cured by heating the sample in air. The cured resin-silica composite was treated at 700°C, in an inert atmosphere of N₂ to obtain the silica-carbon composite. The silica template was removed from the silica-carbon composite by washing it with hydrofluoric acid. The resulting carbon nanocapsules were washed with deionized water until neutrality and dried.

The obtained nanocapsules were dispersed in 50 ml of gold bath adding some drops of ethanol and sonicating during 15 minutes in order to obtain suspensions with 0.5 g/L and 0.25 g/L of carbon nanocapsules. The resulting suspension was analyzed by laser diffraction.

Electrochemical co-deposition procedure⁴. Electrochemical codeposition of gold and nanocapsules was carried out on a rotating disk electrode from the commercial gold bath with dispersed nanocapsules under galvanostatic conditions at an applied constant current density of -1.7 mA/cm². The co-deposition was carried out at different rotation rates (static, 100, 500 and 900 rpm) in the colloidal bath at 30°C. A nickel electrode disk with an exposed area of 1.13 cm² was used as the working electrode. The counter-electrode was a platinum wire and a saturated

calomel electrode reference (0.241 V vs SHE) was used in a three-electrode configuration cell. An Autolab PGSTAT30 potentiostat allowed for performing all electrochemical tests.⁸

Results and Discussion

Nanocapsules characterization and dispersability. The carbon nanocapsules showed a homogeneous morphology consisting of spherical particles with average diameter of 550 nm (**Figure 1**). The TEM image (**Figure 1b**) shows that the capsules have a hollow spherical nucleus with an average diameter of 370 nm and a homogeneous shell with a thickness of 90 nm. Therefore, they were obtained successfully as the inverse replica of the silica template. The SEM image also shows that some of the nanocapsules seem to form agglomerates of 2-4 units. **Figure 1c** shows the nitrogen adsorption-desorption isotherm at 77 K of the carbon nanocapsules, which correspond with a BET specific surface area of 1541 m²/g with a total pore volume of 1.75 cm³/g, which is a contribution of both micro and mesopores. The dispersion of the nanocapsules in the electrolytic gold bath was uniform with an average diameter of around 3 μm, which correspond with a particle aggregation of some nanocapsules.

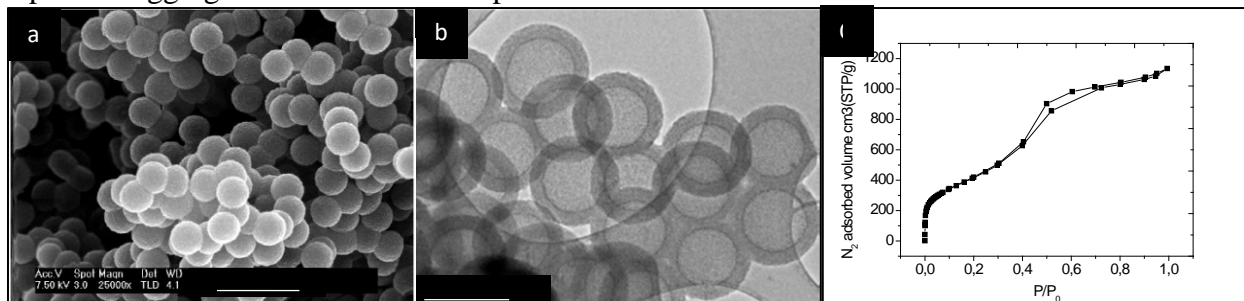


Figure 1. SEM a) and TEM b) images of the synthesized carbon nanocapsules; c) N₂ adsorption-desorption isotherm at 77K of carbon nanocapsules.

Electrochemical co-deposition. The efficiency of the deposition can be shown in **Figure 2a**, where it shows the mass evolution with time of the gold quartz crystal during galvanostatic deposition in two different electrolytic baths, the pure gold and the suspension containing carbon nanocapsules. Higher mass was deposited from the suspension with carbon nanocapsules (up to 30%). It is possible to observe how clusters of particles are covered by gold forming a rounded pattern on the whole surface (**Figure 2b**). The average circular diameter matches very well with the average particle size obtained from the laser diffraction measurements with values between 2.16 and 3.41 μm. **Figure 2b** also shows a FIB cross-section of one composite coating obtained. It is clearly seen how below the rounded shape, clusters of 3–4 nanocapsules are perfectly incorporated under the Au layer. Likewise, the original morphology of nanocapsules can be clearly distinguished indicating their stability under the deposition conditions. The amount of incorporated carbon nanocapsules was quantified by determining the volume of the clusters from the confocal images, they ranged between 18 and 30 μg and the coverage percentage of the surface was between 10 and 88% depending on the deposition conditions. The results indicate that surface coverage increases with the deposition time, while the average height of the clusters is independent of the duration of the galvanic deposition. On the other hand, the agglomeration of incorporated clusters increases with deposition time, resulting in a slightly higher average circular diameter of those clusters. The highest coverages of 77–88% were obtained for the highest rotation rate (900 rpm).

Gold composites formation has been reported to involve adsorption of ionic species on the surface of the particles in the galvanic bath, diffusion of the charged particles to the cathode, reduction of the adsorbed ions and strong anchoring of the particles to the cathode surface.⁹ Incorporation of carbon nanocapsules into gold can be then described with a three-step model based on the previously proposed by Eroglu et al.¹⁰ and shown in **Figure 2c**: (1) mass transfer of the particles to the electrode surface, (2) adhesion of the capsules onto the surface and (3) incorporation in the growing gold film by gold salt reduction on the capsule surface. In the present work, in which conductive particles are co-deposited with the metal, when the carbon nanocapsules reach the metal surface, they are strongly trapped and gold salt reduces on the nanocapsule surface. There is not a burial mechanism of the particles by the growing reduced metal but a direct reduction of the gold on the adhered capsule surface. This later mechanism makes the incorporation rate much higher than that observed for non-conductive particles.¹⁰ On the other hand, the typical hydrophobic properties of the carbon capsules also favor the gold to be adsorbed onto the carbon surface, thus enhancing its reduction under galvanostatic conditions.

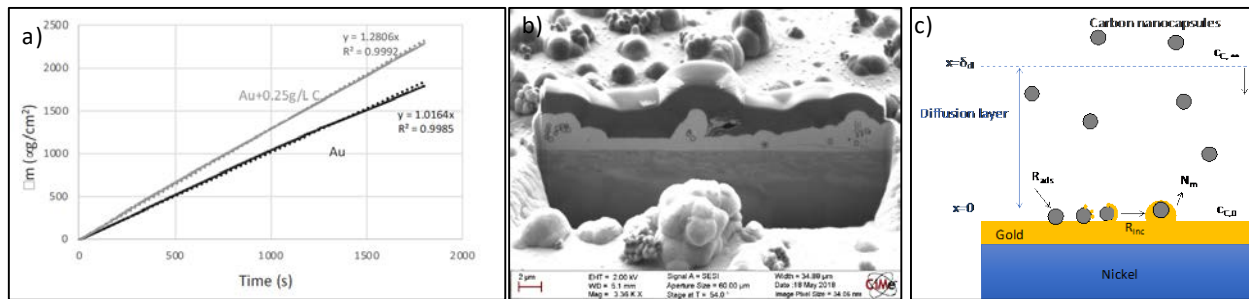


Figure 2. a) Variation of gold thickness with deposition time in the Au and Au+0.25 g/L C nanocapsules suspension; b) FIB cross section of the coating composite 0.25 g/L C; c) Mechanism model adapted from Larson (1984)⁹

Conclusions

Hollow carbon nanocapsules suitable to use in coatings by electrochemical co-deposition of gold were obtained. The nanocapsules had a average diameter of 550 nm and shell thickness of 90 nm with a BET specific surface area of $1541\text{m}^2/\text{g}$ with a total pore volume of $1.75\text{cm}^3/\text{g}$. Higher mass was deposited from the suspension bath when the nanocapsules were included. The nanocapsules maintain their morphology after the co-deposition. Co-deposition mechanisms were found to imply three successive steps: mass transfer of the capsules to the electrode surface, adsorption/adherence of the capsule on the surface and, finally, anchoring of the capsule by the gold electro deposition directly on the capsule surface. The metal film growth directly on the capsule surface makes the incorporation rate much higher than that observed for non-conductive particles. The model allowed rationalizing the influence of particle concentration and mass transport conditions in the particle incorporation in the coating.

Acknowledgment

This research has been financially supported by the Swiss Innovation Agency-Innosuisse within the frame of the CTI project 18738.1 PFNM-NM.

References

1. K. Chaudhari and V. B. Singh, (2018). A review of fundamental aspects, characterization and applications of electrodeposited nanocrystalline iron group metals, Ni-Fe alloy and oxide ceramics reinforced nanocomposite coatings. *Journal of Alloys and Compounds*, 751, 194.

2. C. G. Fink and J. D. Prince. (1928). The Codeposition of Copper and Graphite. *Trans. Am. Electrochem. Soc*, 54, 315.
3. M. Attarchi and S. K. Sadrnezhad. (2009). Pulse reverse electrodeposition of spherical Ni-MWCNT composite spherulites. *IJE Trans. B*, 22B, 161.
4. A. Igual Muñoz, N. Alonso-Morales, J. Palomar, M. A. Gilarranz, and S. Mischler. (2019). *Journal of The Electrochemical Society*, 166 (6) D181-D188.
5. N. Alonso-Morales, M. A. Gilarranz, J. Palomar, J. Lemus, F. Heras, and J. J. Rodriguez. (2013). *Carbon*, **59**, 430
6. N. Alonso-Morales, Cristina Ruiz-García, Jose Palomar, Francisco Heras, Luisa Calvo, Juan J. Rodriguez, and Miguel A. Gilarranz. (2017). *Ind. Eng. Chem. Res.*, 56, 7665
7. R. Santiago, J. Lemus, D. Moreno, C. Moya, M. Larriba, N. Alonso-Morales, M. A. Gilarranz, J. J. Rodríguez, and J. Palomar. (2018). *Chemical Engineering Journal*, 348, 661.
8. C. Valero Vidal, A. Igual Muñoz, C. O. A. Olsson, and S. Mischler. (2012). "Passivation of a CoCrMo PVD Alloy with Biomedical Composition under Simulated Physiological Conditions Studied by EQCM and XPS," *Journal of the Electrochemical Society*, 159,
9. C. Larson (1984). Electrodeposited gold composite coatings Mechanism of formation, mechanical and tribological properties. *Gold Bulletin*, 17, 86.
10. D. Eroglu and A. C. West. (2013). Mathematical Modeling of Ni/SiC Co-Deposition in the Presence of a Cationic Dispersant. *Journal of The Electrochemical Society*, 160.